Journal of Solid State Chemistry 181 (2008) 3044–3050

Contents lists available at ScienceDirect

Journal of Solid State Chemistry

journal homepage: www.elsevier.com/locate/jssc

A simple aqueous metathesis reaction yields new lanthanide monothiophosphates

Nathan J. Takas [a], Lauren E. Slomka [a], Xiaocheng Yang [b], Nancy Giles [b], Jennifer A. Aitken [a,*]

[a] Department of Chemistry and Biochemistry, Duquesne University, Pittsburgh, PA 15282, USA
[b] Department of Physics, West Virginia University, Morgantown, WV 26506, USA

ARTICLE INFO

Article history:
Received 15 April 2008
Received in revised form
23 July 2008
Accepted 30 July 2008
Available online 7 August 2008

Keywords:
Rare earth
Phosphate
Monothiophosphate
Oxythiophosphate
Photoluminescence
Powder X-ray diffraction

ABSTRACT

This paper describes the synthesis and characterization of two, new rare earth monothiophosphate materials, $LaPO_3S \cdot xH_2O$ and $NdPO_3S \cdot yH_2O$, and their properties in comparison to the corresponding orthophosphates prepared by a similar aqueous metathesis reaction. Each of these new materials was found to exist in an amorphous phase similar to a corresponding orthophosphate mineral. The new rhabdophane-type oxythiophosphates were found to display reversible dehydration and rehydration under mild conditions. The materials were found to be thermally unstable. Disproportionation was found to occur at less than 450 °C under vacuum. Sulfur is lost during heating in air between 450 and 650 °C, according to thermogravimetric analysis (TGA) experiments, yielding the orthophosphate. The monothiophosphate hydrates display broad photoluminescence in the visible under excitation by a 325 nm laser. The compounds were also analyzed using differential thermal analysis, FT-IR and UV/vis/NIR spectroscopy.

1. Introduction

Oxythiophosphates are an underrepresented class of materials [1–8] which, although similar in composition to orthophosphates and tetrathiophosphates, still embody a unique family of compounds, with a potentially distinct set of properties [2–4,7,8]. Understanding the relationship between composition and properties in these systems is of fundamental interest because rare earth materials are important to the fields of luminescence and nuclear energy, among others. The early lanthanide phosphates ($LnPO_4$) form two naturally occurring minerals. Monazite (Ln = La to Gd) [9] has a monoclinic structure, incorporates no water, and is thermodynamically favored. Rhabdophane (Ln = La to Dy) is less stable and has a porous hexagonal structure which can be reversibly dehydrated [10]. While both of these minerals have been extensively studied [9–12], the analogous monothiophosphate compounds reported here represent new materials.

Rare earth phosphates are being widely studied for their luminescent properties, which may be useful in optical amplification devices [13], plasma display panels [14], and many other light emitting applications [15]. Depending on the material being studied and the intended application, the luminescence of lanthanide phosphates has been studied from the NIR to the VUV [13,16]. Substitution of the monothiophosphate anion for orthophosphate can provide another degree of freedom in the attempt to develop higher quality phosphors for technological applications.

Many rare earth phosphates are found as naturally occurring minerals [9–12], implying that they are stable on the geologic time scale. This makes rare earth phosphates particularly attractive as a potential nuclear waste storage form [17,18]. Lanthanide phosphates have exceptionally low aqueous solubilities; for instance, lanthanum phosphate has a solubility product constant of merely 3.7×10^{-23} [19]. This very sparing solubility means that radioactive, rare earth nuclear waste stored as its phosphate will not contaminate the local area via water tables near the storage site. We expect lanthanide oxythiophosphates to display similarly useful low solubilities.

In this paper, we describe a simple aqueous metathesis reaction which has produced two new rhabdophane-type lanthanide monothiophosphate hydrates, $LaPO_3S \cdot xH_2O$ and $NdPO_3S \cdot yH_2O$. One of our goals is to demonstrate the similarities and differences between our new rare earth oxythiophosphate materials and the known rare earth phosphates. This is the first step in determining the potential use of these materials. To this end, the materials have been characterized using thermal analysis techniques, diffuse reflectance UV/vis/NIR, photoluminescence and infrared spectroscopy.

* Corresponding author. Fax: +1 412 396 5683.
E-mail address: Aitkenj@duq.edu (J.A. Aitken).

0022-4596/$ - see front matter © 2008 Elsevier Inc. All rights reserved.
doi:10.1016/j.jssc.2008.07.035

2. Experimental

2.1. Synthesis

2.1.1. α-Na_3PO_3S

Alpha-sodium monothiophosphate (α-Na_3PO_3S) was prepared by hydrolysis of $PSCl_3$ (Aldrich, 98%) in an aqueous solution of sodium hydroxide, and subsequently dehydrated by spinning in anhydrous methanol, as described elsewhere [5–7,20].

2.1.2. $LnPO_3S \cdot xH_2O$ and $LnPO_4 \cdot yH_2O$ (where Ln = La, Nd)

Rhabdophane-type lanthanum and neodymium monothiophosphate hydrates and the corresponding phosphate hydrates were prepared by aqueous precipitation [21]. 4 mmol of $LnCl_3$ ($LaCl_3$ Acros 99.99%; $NdCl_3$ Cerac 99.9%) was dissolved in 50 mL of double deionized (DDI) water (18 MΩ) to which was added a solution of either 4 mmol α-Na_3PO_3S or 4 mmol $Na_3PO_4 \cdot 12H_2O$ (Fisher 98%) dissolved in 50 mL DDI water. The sodium monothiophosphate or phosphate solution was added drop-wise at a rate of ~1 mL/min due to the immediate precipitation of the product. The solution was then filtered and energy dispersive spectroscopy (EDS) was used to determine whether further washing of the solid was necessary to remove any NaCl byproduct, which may be present. In most cases, further washing was not necessary; but, in cases where necessary, washing proceeded via sonication of the solid in 50 mL DDI water. The powders yielded by this process were generally white with a slight yellow cast in the case of the lanthanum-containing materials, and a lilac hue in the case of hydrated neodymium-containing materials. The color of the neodymium-containing products took on a deeper blue color upon dehydration.

2.2. Physical measurements

2.2.1. Scanning electron microscopy and energy dispersive spectroscopy

Scanning electron microscopy (SEM) images were obtained using a Tescan VegaXMU scanning electron microscope equipped with an IXRF energy dispersive spectrometer. Samples were prepared on double-sided carbon tape adhered to an aluminum stub. The SEM was operated at 20 kV with a hot tungsten filament. X-ray maps were obtained over 27 min.

2.2.2. Powder X-ray diffraction

Powder X-ray diffraction (PXRD) patterns were obtained on a PANalytical X'Pert PRO MPD powder X-ray diffractometer with the X'cellerator detector, using copper $K\alpha$ radiation and operating at 45 kV and 40 mA. Samples were prepared by backfilling the sample into the aluminum holder. In the case where only exceptionally small samples were available, such as in the examination of thermal analysis residues, the use of a zero-background, Si wafer sample holder was employed. All diffraction patterns were collected from 2° to 70° in 2θ, using a step size of 0.0170°, at a scan rate of 1.1789°/min with the sample rotating.

2.2.3. Differential thermal analysis

Differential thermal analysis (DTA) was performed using a Shimadzu DTA-50, which was calibrated using a three-point calibration curve based on the melting points of indium, zinc and gold metals. The differential signal was balanced prior to the beginning of each experiment. Data were recorded using the Shimadzu TA60-WS collection program. Experiments were performed at a rate of 10 °C/min. Samples were contained in alumina pans under a static air atmosphere. All DTA samples were referenced against an alumina sample, contained similarly and of comparable mass. Multiple heating and cooling cycles were performed in the DTA experiments to differentiate between reversible and irreversible thermal events. DTA residues were routinely examined using PXRD and EDS.

2.2.4. Thermogravimetric analysis

Thermogravimetric analysis (TGA) was performed using a Shimadzu TGA-50. The instrument was consistently operated in the 20 mg sensitivity setting. TGA data were recorded using the Shimadzu TA60-WS collection program. Samples were ground and placed in Pt crucibles. All samples were heated at a rate of 2 °C/min. Anhydrous samples were measured under a flow of N_2 gas (50 mL/min); hydrated samples were heated in a static air atmosphere. TGA residues were routinely examined using PXRD and EDS.

2.3. Optical spectroscopy

2.3.1. Diffuse reflectance

Diffuse reflectance mid-IR spectra were obtained on a Nicolet Nexus 470 FT-IR *ESP* (Thermo Electron Corp.). Spectra were collected against a standard mirror background. Samples were prepared by loading the ground material into a sample cup. All spectra were obtained as the average of 64 scans from 400 to 4000 cm^{-1}. Data manipulation was performed according to the Kubelka–Munk equation [22].

Diffuse reflectance UV/vis/NIR spectra were obtained using a Cary 5000 UV/vis/NIR spectrometer (Varian) equipped with a Praying Mantis diffuse reflectance accessory (Harrick Scientific Corporation). Barium sulfate was used as a 100% reflectance standard. Samples were prepared by loading the ground material into a sample cup. All spectra were obtained from 2500 to 200 nm at a scan rate of 600 nm/min. Data manipulation was performed according to the Kubelka–Munk equation [22].

2.3.2. Photoluminescence

Photoluminescence (PL) spectra were obtained at room temperature using a 325 nm He–Cd laser. The PL signal was detected using a 0.64 m monochromator and a GaAs photomultiplier tube in photon counting mode. The laser power density at the sample was 0.5 W/cm^2. The powder samples were contained between two sapphire plates with the edges sealed by rubber cement. The intensities of the PL spectra were corrected for the detection system response using a calibrated white-light source.

3. Results and discussion

3.1. Synthesis

Although simple, the synthetic method employed is worthy of some note, as other methods, such as alkali polysulfide fluxes, have proven too harsh to conserve the monothiophosphate anion in the lanthanide system. When attempting to prepare a lanthanum monothiophosphate material in a sodium polysulfide flux, Dorhout et al. found that a disproportionation of the monothiophosphate anion was observed, with the product being sodium lanthanum phosphate thiosulfate [23]. However, we have found that a simple aqueous metathesis, which produces sodium chloride as a byproduct, is able to conserve the monothiophosphate anion to form two new lanthanum and neodymium monothiophosphates.

3.2. Crystallinity and phase

Due to the rapid precipitation method employed and the exceedingly low solubility product constant of the lanthanide monothiophosphates, the products obtained are largely amorphous by PXRD. However, a combination of electron diffraction and dark field TEM images revealed that a small component of the sample exists in nanocrystalline domains (10–20 nm), while the bulk of the sample is indeed amorphous. The PXRD patterns of the as-prepared phosphates can be tentatively matched to reference patterns of rhabdophane-type lanthanide phosphates. Other researchers have produced more crystalline rhabdophane-type orthophosphates by aqueous precipitation methods from acidic solutions [21,24]. However, our synthesis was developed to intentionally avoid acidic environments, due to the sensitivity of the monothiophosphate anion under oxidizing conditions [25].

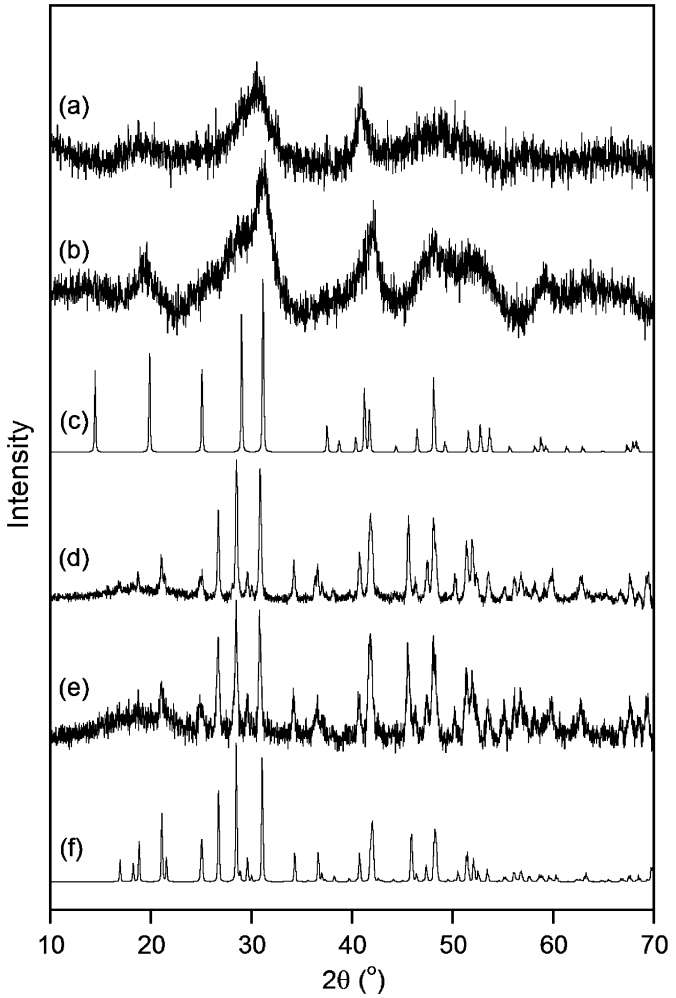

Fig. 1. Powder X-ray diffraction patterns of (a) as-prepared $LaPO_3S$ hydrate, (b) as-prepared $LaPO_4$ hydrate, (c) rhabdophane-type $LaPO_4$ (PDF# 00-046-1439), (d) TGA residue of the as-prepared $LaPO_3S$ hydrate, (e) TGA residue of the as-prepared $LaPO_4$ hydrate, and (f) monazite-type $LaPO_4$ (PDF# 01-073-0188). After TGA analyses, all materials were found to be monazite-type $LaPO_4$ or $NdPO_4$.

Although amorphous, the diffraction patterns of the as-prepared monothiophosphate materials bear strong similarities to the diffraction patterns of the as-prepared phosphates (see Fig. 1a–c).The ability of a monothiophosphate phase to structurally mimic an orthophosphate phase is not unheard of in the literature, and has previously been reported for $H_2Zr(PO_3S)_2$ and $H_2Hf(PO_3S)_2$, which are structural mimics of the equivalent orthophosphates [26]. The IR spectra of the as-prepared materials also support the proposition that these new lanthanum and neodymium monothiophosphates are similar in structure to the rhabdophane-type orthophosphates.

3.3. Infrared

Infrared absorption spectra have held an important role in the debate regarding the structure of rhabdophane-type $LnPO_4$, helping to determine the most appropriate space group for the structure [10]. The utility of the infrared spectra here is primarily to establish evidence for the persistence of the monothiophosphate moiety by observation of the P-S stretch and to establish the rhabdophane-type structure for the monothiophosphate materials (see Table 1) [27]. The observation of the P-S stretch was observed at 496 and 497 cm^{-1} for La and Nd monothiophosphates, respectively, which compare well to the value of 511 cm^{-1} observed in α-Na_3PO_3S.

3.4. Band gaps

Diffuse reflectance UV/vis/NIR revealed the band gaps of the new materials to be 5.35 eV for the as-prepared $LaPO_3S$ hydrate and 5.20 eV for the as-prepared $NdPO_3S$ hydrate (see Fig. 2), which are off-white and faintly lilac powders, respectively. These band gaps are reduced with respect to the orthophosphates, which have band gaps that are too large to be determined using our instrument. The optical spectrum of each of the neodymium rhabdophane-type materials is modified by the superposition of absorptions due to *f–f* transitions [28], as observed in other lanthanide-containing compounds [29–31].

Table 1
Summary of IR data compared with literature values

As-prepared $LaPO_3S$ hydrate	As-prepared $LaPO_4$ hydrate	As-prepared $NdPO_3S$ hydrate	As-prepared $NdPO_4$ hydrate	Assignment[a]
3450,vs	3480,s	3420,vs	3490,s	Water of hydration [32]
1619,s	1633,s	1619,s	1629,s	
	1457,m		1467,m	
	1418,m		1418,m	
1097,s	1164,m	1097,s	1164,m	
1011,m,br	1029,m,br	1006,m,sh	1036,m,br	T_2-A-E (rhab.) [10]
975,m,br	970,m,br		972,m,br	A_1-A-E (rhab.) [10]
670,s	642,m,br	678,m	651,m,br	T_2-2B-A_2 (rhab.) [10]
566,m,br	574,m,br	568,m,br	581,m,br (unresolved)	T_2-A-E (rhab.) [10]
	553,m,br		556,m,br (unresolved)	T_2-2B-A_2 (rhab.) [10]
497,m,br		496,m,br		P-S (α-Na_3PO_3S) [32]

[a] Assignment and mode given are for the material in parentheses. Rhab. designates rhabdophane-type phosphate.

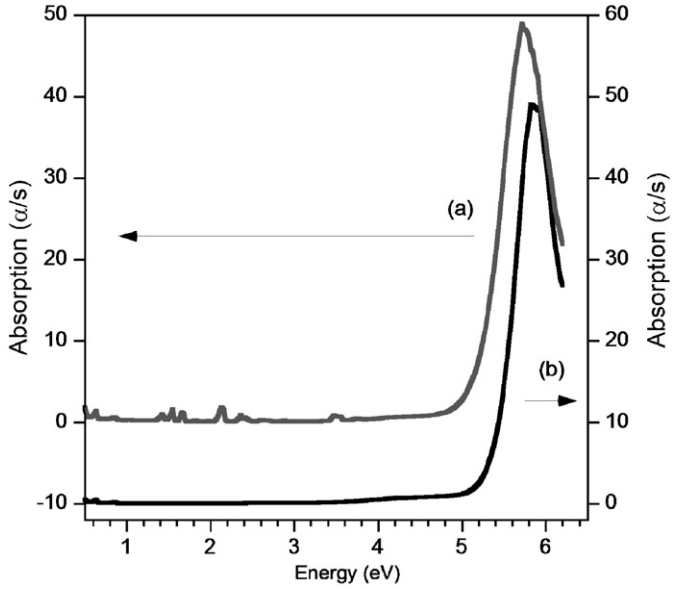

Fig. 2. Optical diffuse reflectance spectra of (a) the as-prepared $NdPO_3S$ hydrate and (b) the as-prepared $LaPO_3S$ hydrate. The Nd spectrum is modified by *f–f* transitions.

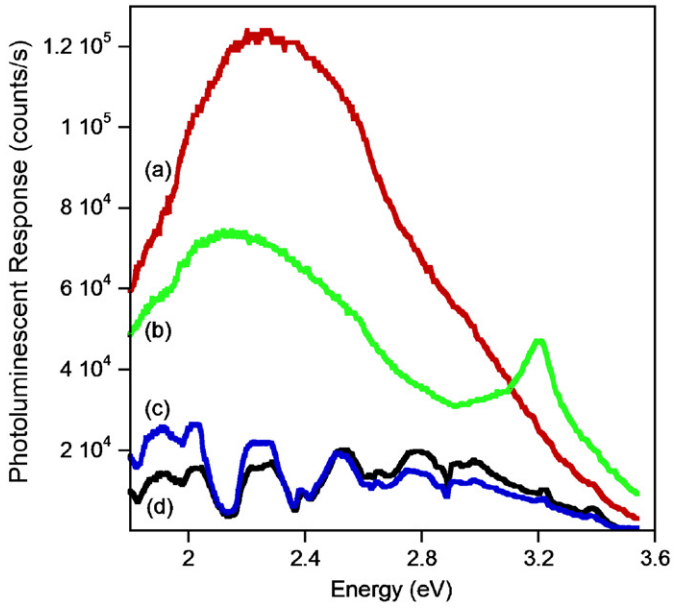

Fig. 3. Photoluminescence spectra of (a) $LaPO_4$ as-prepared hydrate, (b) $LaPO_3S$ as-prepared hydrate, (c) $NdPO_3S$ as-prepared hydrate, and (d) $NdPO_4$ as-prepared hydrate. Both Nd spectra are modified by absorptions arising from *f–f* transitions.

3.5. Photoluminescence

PL spectra reveal that the photoluminescent intensity of the lanthanide monothiophosphate materials is comparable to that of the orthophosphates (see Fig. 3). The sulfur substitution seems to have given rise to an additional broad peak, centered at 3.205 eV in the PL spectrum of $LaPO_3S$ hydrate which may also appear in the other prepared materials with greatly reduced intensity. The PL spectrum of each of the neodymium rhabdophane-type materials is again modified by the superposition of *f–f* transitions [28–31]. One may readily observe that the net intensity of the as-prepared $LaPO_3S$ hydrate is noticeably less than the corresponding orthophosphate material, while the PL response of the Nd-containing materials are largely similar. This difference in the PL response of the La-containing materials may be due to the varied level of hydration of the two materials (see Section 3.6) [32–34]. The total level of hydration of $LaPO_3S$ hydrate is 1.34 times greater than that of $LaPO_4$ hydrate. The total integrated photoluminescent intensity of $LaPO_3S$ hydrate is 1.46 times less than that of $LaPO_4$ hydrate. Further investigation is needed to determine the specific origins of the observed photoluminescent behavior.

3.6. Hydration and thermal stability in air

The rhabdophane-type lanthanide phosphates are known to contain a variable amount of water, cited in the literature as containing 0.5–3.0 molar equivalents [35–39]. The $LnPO_3S$ hydrate

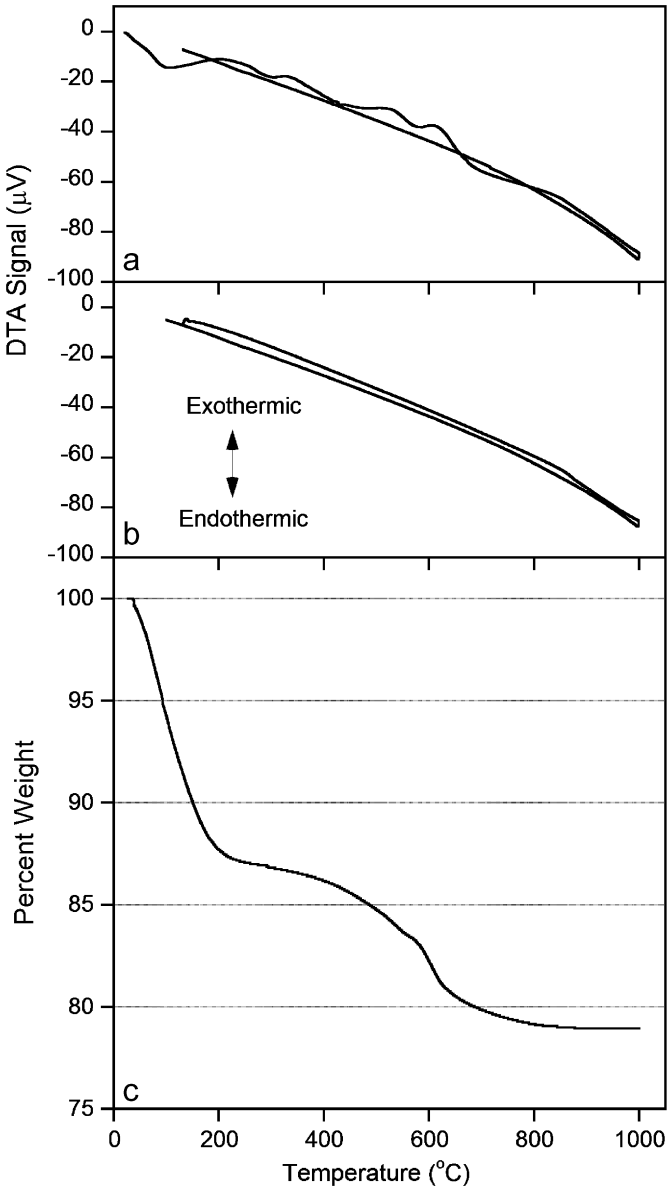

Fig. 4. (a) First DTA cycle of the oxidation of as-prepared $LaPO_3S$ hydrate carried out under a static air atmosphere. Dehydration occurs as an endothermic event up to ~150 °C. Disproportionation and conversion to monazite-type $LaPO_4$ occur as a series of irreversible thermal events from 300 to 850 °C. (b) Second DTA cycle showing no reversible thermal events. (c) The TGA weight loss profile of the as-prepared $LaPO_3S$ hydrate carried out under a static air atmosphere showing three distinct weight loss events.

Table 2
Summary of TGA weight loss data

Material	Dehydration (1st weight loss) (%)	Moles of water lost	Loss of sulfur with gain of oxygen (2nd and 3rd weight losses) (%)	Calculated value for 2nd and 3rd weight losses (%)[a]
$LaPO_3S \cdot xH_2O$	15.65	$-2.57\ H_2O$	5.42	5.42
$NdPO_3S \cdot yH_2O$	13.49	$-2.27\ H_2O$	7.47	5.42
$LaPO_4 \cdot xH_2O$	12.80	$-1.91\ H_2O$	–	–
$NdPO_4 \cdot yH_2O$	14.25	$-2.26\ H_2O$	–	–
Dehydrated $LaPO_3S$	–	–	7.89	6.43
Dehydrated[b] $NdPO_3S$	2.397	$-0.35\ H_2O$	7.65	6.29
Rehydrated $LaPO_3S \cdot H_2O$	5.80	$-0.86\ H_2O$	6.07	6.05
Rehydrated $NdPO_3S \cdot H_2O$	4.176	$-0.99\ H_2O$	8.22	5.88

[a] This column of data were generated by assuming a stoichiometric formula for the compounds.
[b] While efforts were made to prevent rehydration of the sample during preparation for TGA experiments, a small amount of water was absorbed prior to beginning of the TGA experiment.

and $LnPO_4$ hydrate materials produced in this work are no exception, as TGA of the as-prepared products in a static air atmosphere reveals an early weight loss corresponding to loss of water from room temperature to ~200 °C (see Fig. 4c, Table 2). Additionally, each of the as-prepared monothiophosphate materials displays a second and third weight loss, from 450 to 550 °C, and from 550 to 650 °C. The sum of these losses corresponds to the loss of sulfur with a concomitant addition of oxygen. These evaluations are based on EDS and PXRD patterns of the TGA residues. EDS analyses of the TGA residues reveal an absence of sulfur from the materials and PXRD patterns of the post-TGA residues show the materials to be phase-pure monazite-type $LnPO_4$ (see Fig. 1d–f); this confirms that a phase transition does occur as a thermal event [39], but is nonspecific as to the temperature of the event and whether or not it precedes disproportionation.

To further test the assignment of the two weight loss events, a sample of each of the $LnPO_3S$ hydrate samples was dried in an oven at 150 °C for several hours. Thermogravimetric analyses of these materials were obtained under N_2 flow to minimize the possibility of rehydration during the early stages of the experiment. Indeed only the second and third weight losses were then observed (see Table 2). Having established that 150 °C is sufficient to cause the complete removal of the water from the substances, a sample of each of the $LnPO_3S$ hydrate materials was again dried in an oven at 150 °C for several hours. The samples were then allowed to rehydrate by exposure to ambient laboratory conditions for several days (relative humidity ~20%). Thermogravimetric analyses of the materials were again performed and the materials were now found to display similar weight loss events as the original samples; however, the hydration of each of the materials was found to have been reduced to approximately one molar equivalent of water (see Table 2).

DTA examination of the disproportionation and oxidation processes in air revealed that the disproportionation and phase transition to monazite-type $LaPO_4$ occur from approximately 300 to 800 °C (see Fig. 4a,b). The transformation from rhabdophane to the thermodynamically favored monazite is exothermic in the phosphate system [24,39]; however, the monothiophosphate compounds also undergo disproportionation, which convolutes the assignment of thermal events. Dehydration has been established as the first endothermic event, which ends before 200 °C, and oxidation has been established as the third and/or fourth events based on correlations with the TGA data (see Fig. 4).

3.7. Thermal stability of dehydrated samples in Vacuo

The rhabdophane phase, in the orthophosphate system, is only a metastable phase; the monoclinic monazite structure is the more thermodynamically stable phase. Rhabdophane-type lanthanide phosphates convert thermally to the stable monazite structure between 500 and 900 °C as an irreversible exothermic process [24,39]. Therefore, an attempt was made to thermally convert the rhabdophane-type monothiophosphate phases to the corresponding monazite-type phases by heating aliquots of the dehydrated rhabdophane $LnPO_3S$ to 1000 °C in a furnace under static vacuum [39]. This process resulted in disproportionation; the PXRD patterns of the products were found to exactly match those of monazite-type $LnPO_4$. To investigate this process more carefully, a series of $LaPO_3S$ samples were dehydrated by heating in air to 150 °C, sealed under vacuum and heated to maximum temperatures of 150, 300, 450, 600, 750, and 900 °C. While X-ray maps of the 300 °C sample indicated that the sample was single phase, X-ray maps of the 450 °C sample showed that the material had disproportionated. X-ray maps of the 900 °C sample clearly showed phase segregation, as the sulfur was present in islands which also contained lanthanum and phosphorus (see Fig. 5).

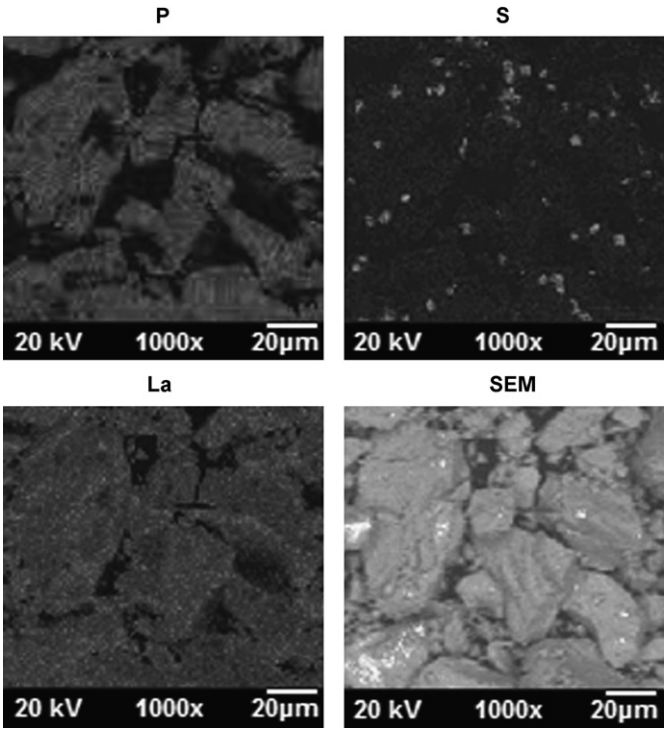

Fig. 5. Elemental maps and SEM image of dehydrated $LaPO_3S$ heated to 900 °C under vacuum showing phase segregation at high temperatures.

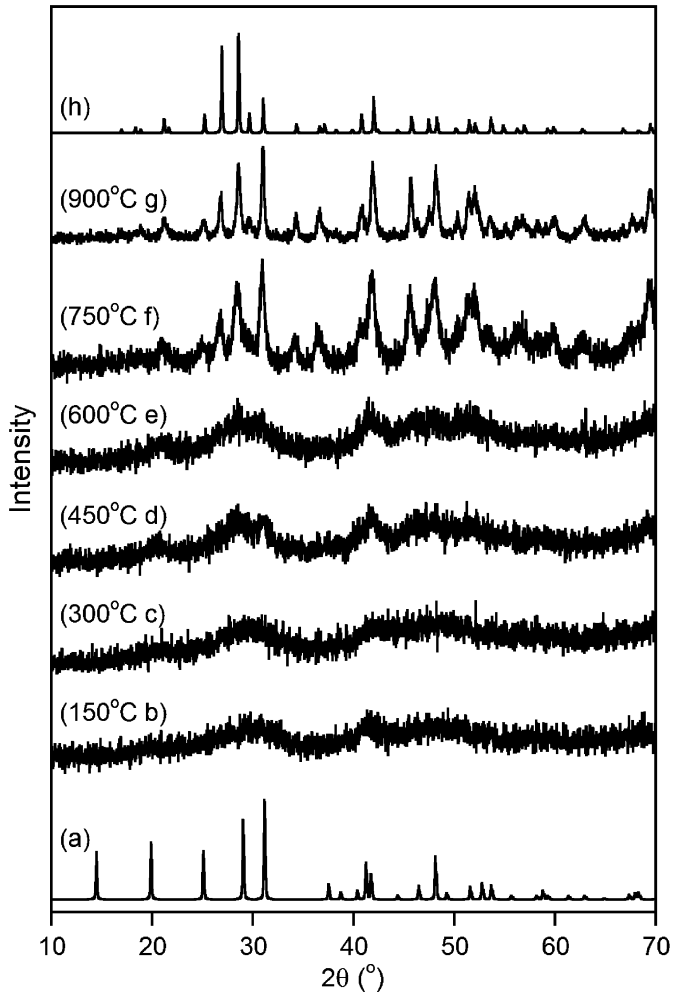

Fig. 6. Ex-situ PXRD diffraction patterns of dehydrated $LaPO_3S$ heated under vacuum to various temperatures: (a) rhabdophane-type $LaPO_4$ (PDF# 00-046-1439), (b) 150 °C, (c) 300 °C, (d) 450 °C, (e) 600 °C, (f) 750 °C, (g) 900 °C, and (h) monazite type $LaPO_4$ (PDF# 00-012-0283).

PXRD patterns of the residues revealed sharpened diffraction peaks for samples heated to 750 and 900 °C (see Fig. 6). The PXRD pattern of these samples matched that of monazite-type lanthanum phosphate; however, the patterns did not indicate any secondary crystalline component. Therefore, the identity of the sulfur-containing species remains unknown; however, it seems reasonable to suppose that it may be $LaPS_4$ based on the EDS results.

Several attempts were made to observe this disproportionation process under static vacuum by DTA; however, the DTA ampoules burst every time at around 600 °C. It is interesting to note the temperature at which the DTA ampoules failed, as this corresponds to the temperature range during which the samples lose sulfur and gain oxygen during TGA experiments in air. The thermal stability of the material therefore, does not seem to be greatly affected by the presence of air. The lack of an effect by air on the thermal stability of the materials may mean that disproportionation in air may be similar to that observed under vacuum. The proposition that the second endothermic DTA event (300–400 °C) may correspond to disproportionation could not be tested unambiguously, as the material has already begun to lose mass in this region by TGA experiments.

4. Conclusions

A soft and simple aqueous metathesis has been used to prepare two new lanthanide oxythiophosphate hydrates which are mimics of the naturally occurring orthophosphate mineral rhabdophane. Hydration and IR support that the new monothiophosphate materials are structurally related to the mineral rhabdophane. At low temperatures, dehydration and rehydration may be cycled. Both materials were found to retain the monothiophosphate anion up to a minimum temperature of 300 °C under vacuum, however, at higher temperatures, disproportionation led to islands of an unknown sulfur-containing phase and a phase transition to monazite-type $LnPO_4$. The temperature of the phase transition which finally yields monazite-type $LnPO_4$ cannot be pinpointed and may occur in concert with the oxidation process. The marked similarity of the chemistry of the trivalent lanthanides encourages us to predict that other lanthanide monothiophosphates may be formed by similar metathesis reactions. Additionally, this method's simplicity makes it a desirable synthetic option for the discovery of other new oxythiophosphate materials which may be prone to decomposition or disproportionation under any but the gentlest of conditions.

Acknowledgments

NJT, LES and JAA thank the Bayer School of Natural and Environmental Sciences for funding. The powder X-ray diffractometer was purchased with funds from the National Science Foundation (Grant no. DUE-0511444), LES thanks the Noble Dick Fund for a summer research fellowship. NG and XY were supported by the National Science Foundation (Grant no. DMR-0508140).

Appendix A. Supplementary data

Supplementary data associated with this article can be found in the online version at doi:10.1016/j.jssc.2008.07.035.

References

[1] K.K. Palkina, S.I. Maksimova, N.T. Chibiskova, T.A. Tripol'skaya, G.U. Wolf, T.B. Kuvshinova, Izv. Akad. Nauk SSSR, Neorg. Mater. 27 (1991) 1028–1031.
[2] M. Pompetzki, M. Jansen, Z. Anorg. Allg. Chem. 629 (2003) 1929–1933.
[3] M. Pompetzki, L. van Wuelen, M. Jansen, Z. Anorg. Allg. Chem. 630 (2004) 384–388.
[4] M. Pompetzki, R.E. Dinnebier, M. Jansen, Solid State Sci. 5 (2003) 1439–1444.
[5] N.J. Takas, J.A. Aitken, Inorg. Chem. 45 (2006) 2779–2781.
[6] N.J. Takas, J.A. Aitken, J. Solid State Chem. 180 (2007) 2034–2043.
[7] A.E. Gash, P.K. Dorhout, S.H. Strauss, Inorg. Chem. 39 (2000) 5538–5546.
[8] I.A. Stenina, A.D. Aliev, P.K. Dorhout, A.B. Yaroslavtsev, Inorg. Chem. 43 (2004) 7141–7145.
[9] E.N. Silva, A.P. Ayala, I. Guedes, C.W.A. Paschoal, R.L. Moreira, C.-K. Loong, L.A. Boatner, Opt. Mater. 29 (2006) 224–230.
[10] H. Assaaoudi, A. Ennaciri, A. Rulmont, Vib. Spectrosc. 25 (2001) 81–90.
[11] K. Wang, J. Zhang, J. Wang, C. Fang, W. Yu, X. Zhao, H. Xu, J. Appl. Crystallogr. 38 (2005) 675–677.
[12] Y. Hikiichi, C.F. Yu, M. Miyamoto, S. Okada, J. Alloy Compd. 192 (1993) 102–104.
[13] J.-K. Jung, J.-S. Oh, S.-I. Seok, T.-H. Lee, J. Lumin. 114 (2005) 307–313.
[14] R.P. Rao, D.J. Devine, J. Lumin. 87–89 (2000) 1260–1263.
[15] B. Moine, G. Bizarri, Opt. Mater. 28 (2006) 58–63.
[16] Y. Wang, C. Wu, J. Wei, J. Lumin. 126 (2007) 503–507.
[17] B. Glorieux, R. Berjoan, M. Matecki, A. Kammouni, D. Perarnau, Appl. Surf. Sci. 253 (2007) 3349–3359.
[18] R.C. Ewing, L.-M. Wang, Rev. Miner. Geol. 48 (2002) 673–699.
[19] M. Kawase, T. Suzuki, K. Miura, Chem. Eng. Sci. 62 (2007) 4875–4879.
[20] S.K. Yasuda, J.L. Lambert, Inorg. Syn. 5 (1957) 102–104.
[21] S. Lucas, E. Champion, D. Bregiroux, D. Bernache-Assollant, F. Audubert, J. Solid State Chem. 177 (2004) 1302–1311.
[22] P. Kubelka, F. Munk, Z. Tech. Phys. 12 (1931) 593–601.

[23] M.G. Zhizhin, H.A. Pounds, F.M. Spiridonov, L.N. Komissarova, P.K. Dorhout, J. Alloy. Compd. 418 (2006) 90–94.
[24] R. Kijkowska, Thermochim. Acta 404 (2003) 81–88.
[25] E. Thilo, E. Schone, Z. Anorg. Chem. 259 (1949) 225–232.
[26] A. Clearfield, J.A. Stynes, J. Inorg. Nucl. Chem. 26 (1964) 117–129.
[27] G. Socrates, Infrared Characteristic Group Frequencies: Tables and Charts, Wiley, New York, 1994.
[28] F.A. Cotton, G. Wilkinson, C.A. Murillo, M. Bochmann, Advanced Inorganic Chemistry, Wiley, New York, 1999, pp. 1108–1129.
[29] G.B. Jin, E.S. Choi, R.P. Guertin, J.S. Brooks, T.H. Bray, C.H. Booth, T.E. Albrecht-Schmitt, J. Solid State Chem. 7 (2007) 2129–2135.
[30] G.W. Burdick, C.K. Jayasankar, F.S. Richardson, Phys. Rev. B 50 (1994) 16309–16325.
[31] Y. Hasegawa, Y. Wada, S. Yanagida, J. Photochem. Photobiol. C 5 (2004) 183–202.
[32] G.M. Davies, R.J. Aarons, G.R. Motson, J.C. Jeffery, H. Adams, S. Faulkner, M.D. Ward, Dalton Trans. (2004) 1136–1144.
[33] G.M. Davies, S.J.A. Pope, H. Adams, S. Faulkner, M.D. Ward, Inorg. Chem. 44 (2005) 4656–4665.
[34] A. Beeby, I.M. Clarkson, R.S. Dickins, S. Faulkner, D. Parker, L. Royle, A.S. de Sousa, J.A.G. Williams, M. Woods, J. Chem. Soc. Perkin Trans. 2 (1999) 493–503.
[35] J.F.W. Bowles, D.G. Morgan, Miner. Mag. 48 (1984) 146–148.
[36] C.R. Patra, G. Alexandra, S. Satra, D.S. Jacob, A. Gedanken, A. Landau, Y. Gofer, New J. Chem. 29 (2005) 733–739.
[37] S. Gallini, J.R. Jurado, M.T. Colomer, Chem. Mater. 17 (2005) 4154–4161.
[38] V. Buissette, M. Moreau, T. Gacoin, J.-P. Boilot, J.-Y. Chane-Ching, T. Le Mercier, Chem. Mater. 16 (2004) 3767–3773.
[39] R.G. Jonasson, E.R. Vance, Thermchim. Acta 108 (1986) 65–72.